GLOBAL LUNAR WRINKLE RIDGE IDENTIFICATION AND ANALYSIS. T.J. Thompson[1], M.S. Robinson[1], T.R. Watters[2], and M.B. Johnson[2], [1]School of Earth and Space Exploration, Arizona State University, 1100 S. Cady, Tempe, AZ 85287 (tjthomp9@asu.edu); [2]Center for Earth and Planetary Studies, National Air and Space Museum, Smithsonian Institution, Washington, DC 20560, USA.

Introduction: Wrinkle ridges are positive relief tectonic landforms first discovered on the Moon [cf. **1,2**] and later found on other terrestrial bodies. Comparison of lunar mare wrinkle ridge morphology and Earth analog folding and thrust-fault features in the Columbia Plateau basalts indicate the mare wrinkle ridges are the result of compressional stresses acting on mare basalts [**2,3**]. Wrinkle ridges are complex structures with primary, secondary, and tertiary ridges, with equally complicated origin hypotheses. Wrinkle ridges are readily identifiable within the Lunar Reconnaissance Orbiter Camera (LROC) Wide Angle Camera (WAC) [**4**] mosaics and the GLD100 Digital Terrain Model (DTM) at 100 meter pixel scale [**5**]. The mare regions contain wrinkle ridges ranging in length from hundreds of meters to many kilometers, with a variety of strikes and sometimes a package of related features that form an assemblage [**1,2,3**]. From the WAC map products we produced a near-global dataset of wrinkle ridge features that complements the growing body of global lunar geologic data including the lobate scarp tectonic feature dataset [**6**]. Wrinkle ridges are important for lunar geology because they are products of large scale stress fields. In an ideal model the axis of compressional stress is perpendicular to the long axis of the thrust fault surface expression, thus indicating the orientation of the stress field at the time of formation.

Methods: QGIS open source GIS software was used to digitize the spatial extents of the wrinkle ridges. Terrain analysis functions generated hillshade maps from different Sun directions at a constant solar elevation. Cycling these hillshade maps minimizes identification errors due to solar azimuth. Coupling these data sources (image mosaic, DTM, hillshade maps) allows the digitizer to model light from different directions to emphasize the principal structure of the wrinkle ridge assemblage such that multiple parts of the same structure are not digitized. For smaller or subtle features we applied various stretches to the topography and created hillshades with solar azimuth perpendicular to feature strike. This dataset traces the centerline of the wrinkle ridge assemblage, which is sometimes composed of a broad arch and sharp ridge and sometimes secondary ridges of smaller magnitude [i.e. **3**]. Without care it is possible to interpret multiple parts of the same assemblage as individual features or incorrectly interpret the flanks of a broad arch as two individual ridges. Once the polyline shapefile has been digitized and reviewed, QGIS software vector tools were used for basic geoprocessing. The wrinkle ridges features were separated into individual shapefiles based on the mare region they occur within using the clipping tool in QGIS. A MATLAB© script reads in the wrinkle ridges shapefile, calculates the azimuths, multiplies them by a weight (segment length divided by polyline length), and generates the length normalized azimuth for each polyline by summing the length weighted azimuths of each line segment within the polyline. Thus longer segments have a greater effect on the azimuth calculation than short segments like small steps. This metric allows basic tests of wrinkle ridge orientation in from different mare-to-mare.

Dataset Overview: The current state of the wrinkle ridge dataset (**Fig. 1**) includes 5945 polyline features distributed amongst the various mare. The largest numbers of features (2062) are found in the largest mare region, Oceanus Procellarum. Note that there are no features digitized at the far northern or southern reaches of the mosaic likely due to the absence of mare in these regions.

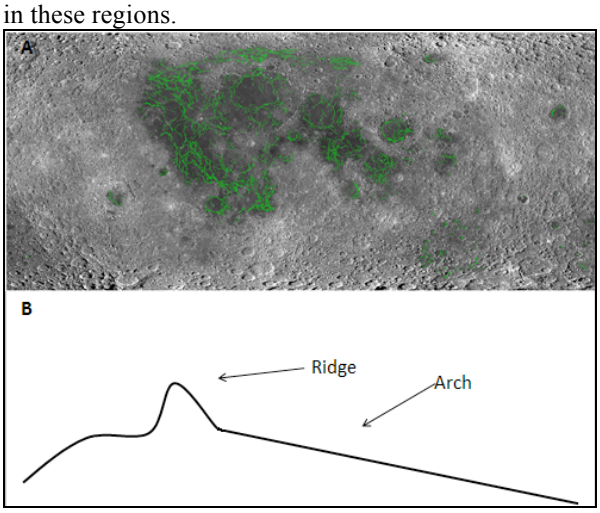

Fig. 1. (A) Distribution of wrinkle ridges (green) across the Wide Angle Camera (WAC) mosaic. (B) Idealized profile view of a wrinkle ridge featuring a broad arch and a comparatively sharp ridge.

Preliminary Investigation: A preferred orientation of a set of fault features indicates some predominant stress field. For a polyline feature composed of a number of segments (sequential node pairs) of varying orientation and length requires designing a specific metric to test an orientation hypothesis. One way to get a metric for polyline orientation is to sum the azimuths

of the segments weighted by multiplying the fraction of segment length to polyline length. Thus small departures from the mean azimuth of the wrinkle ridge are not overly valued. Each polyline may also be described by a length. For a set of lines with random orientations one would expect the sum of the line lengths for each azimuth to be zero since there is an equal probability of both a positive or negative value of the same magnitude. If north is zero degrees, east is positive 0° to 90°, west is 0° to -90° (for biaxial orientation data), there should be a uniform distribution of line lengths as a function of azimuth described in this way assuming the distribution of orientations is uniform. If there is a bias the mean azimuth of the full set of features will be positive or negative. Calculating this for our dataset reveals a slight northwest bias in feature orientation of -2.23º degrees. This is seemingly consistent with the results of a polygon feature wrinkle ridges dataset produced by Yue et al. [**7**] with a value of -1.99º with about half the number of features (2839). Not all mare are circular shaped. Perhaps less circular mare show less uniformly distriubuted length normalized polyline azimuths. Thus the mare polygons shapefile was used to group the wrinkle ridges by the mare they occur within. The average of the polyline azimuths for each mare are then compared (Table 1). Even the circular mare regions such as Imbrian, Serenitatis, Crisium, Nectaris, and Humorum have non-zero mean azimuths across the feature count in those regions. The negative values for Serenitatis, Nectaris, Humorum, and Procellarum are consistent with the general northwestern feature strike found in [**7**], but Crisium, Imbrium, and Frigoris did not fit the general global assumption. Consistent with basin long-axis orientation affecting the stress field, Oceanus Procellarum displays the largest negative mean azimuth, and over the largest number of features of these subsets indicating this mare contributes strongly to the overall slightly northwestern orientation bias.

Mare Name	Mean Azimuths	Count
Imbrium	5.2	445
Serenitatis	-1.9	117
Crisium	0.9	297
Nectaris	-2.6	56
Humorum	-0.7	147
Procellarum	-10.2	2062
Frigoris	1.6	694

Table 1. Mean of the length normalized azimuths and polyline counts for several mare areas.

Future Directions: Generating global geologic datasets including basin age maps, tectonic features, and volcanic features, aids in tying together case studies to put together a holistic geologic history of the Moon. As a compliment to the wrinkle ridge global dataset, we have also begun generating a depression (negative relief feature) dataset **(Fig. 2)** that includes the global distribution of extensional graben features, sinuous rilles, and floor fractured craters. With respect to the stress field story and the mascon model [**8,9**] contractional strain inside the mascon basins can be contrasted with extensional strain on the margins and outside the boundary of the basins. Thus for the ideal cases there should be coincident gravity highs, wrinkle ridges, and extensional grabens concentrically oriented. Having these datasets ready and available will aid in a deeper understanding of the lunar stress field and geologic history.

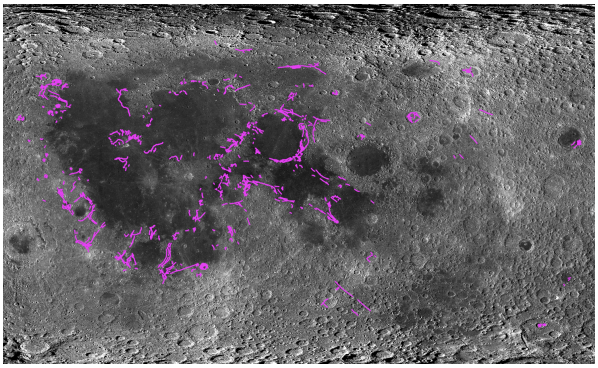

Fig. 2. Pink lines representing a digitized depressions shapefile including sinuous rilles, grabens, and floor fractures atop WAC mosaic

Additional Information: The WAC global mosaic, WAC DTM, mare shapefile, and lobate scarps shapefiles mentioned in this abstract, as well as a tremendous amount of other LRO data may be downloaded from http://lroc.sese.asu.edu/archive and the shapefile for the mare may be downloaded from http://wms.lroc.asu.edu/lroc/view_rdr/SHAPEFILE_LUNAR_MARE

References: [1] Bryan, W.B. (1973) *PLSC* 4th, pp. 93-106. [2] Plescia, J.B. and M.P. Golombek (1986) *Geol. Soc. Am Bull.*, 97, 1289-1299. [3] Watters T.R. (1988) *JGR, 93,* 10236–10254. [4] Robinson M.S. et al. (2010) *Space Sci. Rev., 150,* 81-124. [5] Scholten F. et al. (2012) *JGR, 117,* E00H17. [6] Watters T.R. (2010) *Science, 329,* 936-940. [7] Yue Z. et al. (2015) *JGR, 120,* 978-994. [8] Phillips R.J. et al. (1972) *JGR, 77, 7106-7114.* [9] Freed A. M. et al. (2001) *JGR*, *106,* 20603-20620.